VERSITA

CELLULAR & MOLECULAR BIOLOGY LETTERS
Volume 12 (2007) pp 51 - 69
http://www.cmbl.org.pl

DOI: 10.2478/s11658-006-0059-6

Received: 18 April 2006
Revised form accepted: 09 August 2006
Published online: 24 November 2006

SPECTROSCOPIC STUDIES OF D-α-TOCOPHEROL CONCENTRATION-INDUCED TRANSFORMATION IN EGG PHOSPHATIDYLCHOLNE VESICLES

KRZYSZTOF DWIECKI[1], PAWEŁ GÓRNAŚ[1], AGNIESZKA WILK[3], MAŁGORZATA NOGALA-KAŁUCKA[2] and KRZYSZTOF POLEWSKI[1]*
[1]Department of Physics, ul. Wojska Polskiego 38/42, 60-637 Poznań, Poland,
[2]Department of Biochemistry and Food Analysis, ul. Mazowiecka 48, 60-623 Poznań, Poland; August Cieszkowski Agricultural University, Poznań, Poland,
[3]Institute of Physics, A. Mickiewicz University, 61-614 Poznań, Poland

Abstract: The effects of embedding up to 60 mol% of α-tocopherol (α-Toc) on the morphology and structure of the egg phosphatidylcholine (PC) membrane were studied using spectroscopic techniques. The resulting vesicles were subjected to turbidometric and dynamic light scattering measurements to evaluate their size distribution. The α-Toc intrinsic fluorescence and its quenching was used to estimate the tocopherol position in the membrane. Optical microscopy was used to visualize morphological changes in the vesicles during the inclusion of tocopherol into the 2 mg/ml PC membrane. The incorporation of up to 15 mol% of tocopherol molecules into PC vesicles is accompanied by a linear increase in the fluorescence intensity and the simultaneous formation of larger, multilamellar vesicles. Increasing the tocopherol concentration above 20 mol% induced structural and morphological changes leading to the disappearance of micrometer-sized vesicles and the formation of small unilamellar vesicles of size ranging from 30 to 120 nm, mixed micelles and non-lamellar structures.

---

* Author for correspondence; e-mail: polewski@au.poznan.pl

Abbreviations used: α-Toc – D-α-tocopherol; ACR – acrylamide; DLS – dynamic light scattering; DMPC – dimyristoyl phosphatidylcholine; DPPC – dipalmitoyl phosphatidylcholine; GUV – giant unilamellar vesicle; GMV – giant multilamellar vesicle; GLV – giant lamellar vesicle; KI – potassium iodide; K_D – dynamic fluorescence quenching constant; K_{SV} – Stern-Volmer quenching constant; LMV – large multilamellar vesicle; NMR – nuclear magnetic resonance; PC – L-α-phosphatydylcholine; SSBV – small single-bilayer vesicle; SUV – small unilamellar vesicle; V – static fluorescence quenching constant

Key words: Egg phosphatidylcholine, Tocopherol, Fluorescence, Vesicles, Optical microscopy, Dynamic light scattering

INTRODUCTION

Vitamin E is a generic name for a mixture of different types of tocopherols, the most abundant of which is D-α-tocopherol (α-Toc), a biologically active lipid-soluble antioxidant. The chromanol ring of α-Toc is thought to be located in the polar region of the membrane, where the phenoxyl hydrogen group is hydrogen-bonded to the carbonyl group of the lipid. The interaction of tocopherol with other membrane constituents has an effect on membrane stability. The location of α-Toc in the membrane and its interaction with the membrane components may determine its biological activity. As shown in reported studies, the presence of α-tocopherols in the model membrane improves acyl chain order, decreases fluidity in liquid crystalline bilayers, and reduces the phase transition temperature of gel to liquid-crystalline state [1-3]. There are reports showing that the presence of tocopherol in a suspension of cells promotes fusion [4, 5]. In model studies with DPPC and DPMC membranes, it has been shown that the presence of tocopherol in the membrane stabilizes its structure [6, 7] via the formation of complexes with membrane lipids [8-10]. The tocopherol concentration in the above-described experiments was usually between 2 and 8 mol%, and never higher than 12 mol%.

In biological membranes, tocopherol concentration rarely exceeds 2 mol%. However, there are zones of much higher α-Toc concentration. For example, upon supplementation with vitamin E or during encapsulation in liposomes, the α-Toc concentration may reach 80% [11]. This raises a number of questions. How does an increased amount of vitamin E interact with lipid membranes? What are the limiting factors for membrane saturation with vitamin E? What is the role of the excess tocopherol molecules in the system? Increasing tocopherol concentration in a membrane can be expected to lead to new interactions, which may disturb the morphology and structure of the membrane. Incorporation of high (above 10 mol%) molar fractions of tocopherols into a PC membrane was investigated using X-ray and freeze-fracture electron microscopy [12, 13], which revealed the formation of a ripple phase with tocopherol-enriched domains. In spectroscopic studies [14] using fluorescent probes, the presence of 20 mol% of α-Toc in DPPC membranes was found to reduce acyl chain mobility and interfacial polarity. The formation of domain structures in alpha tocopherol-enriched PC membranes has been clearly evidenced by impedance spectroscopy [15]. Another technique used for detecting submicrometer range domains in membranes is atomic force microscopy [16-18].

Giant vesicles were used as a model of biomembranes suitable for optical microscopy detection [19] due to their resemblance to cell membranes compared to supported bilayers and monolayers, which are prone to artifacts. Giant liposomes (in the form of unilamellar or multilamellar vesicles) were used as

model membrane systems, mainly to study the antioxidant properties of tocopherols and other antioxidants by means of spectroscopic techniques such as fluorescence, confocal microscopy, fluorescence lifetimes, fluorescence energy transfer and NMR [14, 20-25]. The investigations were focused on the antioxidation processes as well as on changes in the structural and physico-chemical properties of the membrane bilayer.

We applied spectroscopic methods in order to detect and measure the changes in the membrane at the molecular and microscopic levels. Fluorescence spectroscopy and fluorescence quenching are suitable techniques for providing information on the location of α-Toc in micellar and lipid systems, mainly because of fluorescence spectrum sensitivity to the microenvironment.

No single particle-sizing method can be sufficient to describe the complete particle size distribution in the investigated system, as the dimensions of the aggregates formed vary widely, ranging from nanometers to tens of micrometers. We used two methods in which different properties of dispersed particles are measured in order to estimate their diameter values. One method is dynamic light scattering, a technique widely used for measuring the size distribution of cells, micelles and vesicles in the range from 5 to 1000 nm. The other method, optical microscopy, was applied to directly visualize the formation and the morphological changes in GUV with diameters ranging from a few micrometers to 50 micrometers. Concentration-induced structural and morphological effects in unilamellar and multilamellar PC vesicles due to increasing α-Toc concentration up to 60 mol% were investigated within this study.

MATERIALS AND METHODS

Reagents and vesicle preparation

L-α-phosphatydylcholine (lecithin) of purity > 99% from egg yolk was purchased from Sigma Aldrich (Germany). It is composed of approximately 33% palmitic acid (16:0), 13% stearic acid (18:0), 31% oleic acid (18:1), and 15% linoleic acid (18:2), with other fatty acids being minor contributors, and has an average molecular weight of 768 [26]. The above data indicates that at least 50% of the PC bilayer is composed of unsaturated fatty acids. Lecithin tends to be used as a synonym for phosphatidylcholine (PC), which is the major component of the phosphatide fraction isolated from either egg yolk or soy beans. PC is a mixture of differently substituted sn-glycerol-3-phosphatidylcholine backbones. In PC originating from egg yolk, saturated acyl groups are more common in the sn-1-position, whereas unsaturated fatty acids are dominant in the sn-2-position [27]. Almost all naturally occurring unsaturated fatty acids are entirely of the all-cis-conformation [28].

An external standard of D-α-tocopherol, obtained from Calbiochem (USA), was used as a reference. Acrylamide ACM, potassium iodide KI and $CuSO_4$ were purchased from POCh (Poland).

For the membrane studies, PC and α-Toc were dissolved in chloroform and mixed to obtain the desired molar fractions. Chloroform solutions containing from 2 to 800 μM of D-α-tocopherol in 0.2 mg/ml or 2 mg/ml of PC were dried in nitrogen in order to obtain a thin film on the bottom of the flask. Then the sample was kept under a vacuum to remove traces of solvent. In the preparation of giant multilamelar vesicles (GMV) and large multilamelar vesicles (LMV), a magnetic Heidolph MR 3001 K/EKT 3001 stirrer/heater (Germany) was employed to maintain the preset temperature values. The stirring speed was approximately 700 rpm; vesicles were formed by incubating the dried lipid in distilled water under vigorous vortexing at 22ºC for 5 minutes in nitrogen. After 15 minutes of stirring, the final weight was adjusted with double-distilled water. As the main transition temperature for PC is below 0ºC, such a temperature was used solely in order to obtain a homogeneous and uniform suspension. Two concentrations of the PC membrane, 0.2 and 2 mg/ml, were used in the studies.
Upon water uptake, lecithin forms lamellar closed spherical bilayer vesicles widely ranging in size, depending on the head group type, pH, temperature and hydration [30]. The assignment of the observed structures is based on data from the literature. Small single-bilayer vesicles with a diameter below 20 nm are called SSBV, those up to 100 nm are considered small unilamellar vesicles (SUV), and those up to 1000 nm large unilamellar (LUV) or multilamellar (MLV) vesicles. Vesicles with a diameter exceeding 1 micrometer are referred to as giant lamellar or multilamellar vesicles (GLV).

Fluorescence and absorbance spectra

Fluorescence spectra between 300 nm and 500 nm were measured with a Shimadzu 1501 PC spectrofluorimeter equipped with a thermostatic cuvette holder. The α-Toc emission spectra were measured at an excitation wavelength of 295 nm in a 1 cm cuvette at room temperature, 22ºC. In the quenching studies, the aliquots of quencher stock solutions were added directly to the sample and equilibrated for ten minutes before measurements were taken. All the quencher solutions were freshly prepared before the measurements, and in the case of KI, a small amount of sodium thiosulphate was added to inhibit I^{-3} formation. The correction of acrylamide absorption at 295 nm was applied.
Absorbance spectra in the range from 200 nm to 700 nm were taken with an Ocean Optics S1000 spectrometer. Turbidity was measured at 450 nm on the absorption spectrum. The presented data is based on the results of three to five different sets of experiments.

Dynamic light scattering (DLS)

The experimental setup for the dynamic light scattering measurements consisted of a Helium-Neon laser (Zeiss, HNA 188-S,Germany, $\lambda = 632.8$ nm, operating at 30 mW, linearly polarized light), a goniometer and an ALV-5000E digital correlator (both manufactured by ALV, Langen). The scattered light was collected using a mono-mode optical fiber mounted on the arm of the

goniometer (ALV/SP-125, ALV GmbH, Langen, Germany) and fed into a high quantum efficiency photon-counting avalanche photodiode (APD unit, ALV GmbH, Langen, Germany). The sample temperature was maintained at 20ºC within ± 0.1ºC. Prior to each measurement, the water was filtered (with 0.2 μm Millipore disposable filter units) into dust-free 10 mm cylindrical scattering cells, which were centrifuged at 4000 *g* for 30 minutes to remove air bubbles. The homodyne intensity autocorrelation function was measured at various scattering vector length values (at angles of 30º, 45º, 60º, 90º, 120º and 150º). The inverse Laplace transform (CONTIN) was applied in order to obtain the relaxation time distribution. Independently, the relaxation time values were determined from the triple-exponential fits. The diffusion coefficients were then calculated with the equation:

$$\frac{1}{t} = Dq^2,$$

where t is the relaxation time, D denotes the translation diffusion coefficient, and q is the scattering vector length defined as:

$$|\boldsymbol{q}| = \frac{4\pi n}{\lambda} \sin \theta/2.$$

where θ is the scattering angle and n the refractive index of the solution.
The hydrodynamic radii were calculated using the Stokes-Einstein equation (assuming a spherical shape). Finally, the number-weighted particle radius distribution function was determined from the decay time distribution using the Stokes-Einstein equation [29].

Light microscopy
An AXIO SCOPE 2 Plus light microscope from Zeiss, Germany, equipped with a photographic camera was used. 10 μl of the sample was placed on a microscope cover slip and covered with another one. The pictures were taken in oil immersion with an optical magnification of 100x. Six to ten images of each sample were taken. At each concentration, 3 to 5 samples were prepared on microscopic cover slips. This means that the characteristic image for a given concentration was chosen from 18 to 50 individual frames.

RESULTS

Fluorescence spectra
Intrinsic α-Toc fluorescence provides a sensitive probe of its microenvironment. In hexane, the lowest energy transition of the α-Toc molecule is found at 296 nm; when excited in its absorption band, α-Toc exhibits fluorescence with a maximum at 325 nm. The shape and position of the α-Toc fluorescence maximum in PC is similar to that recorded in hexane, which suggests a similar dielectric microenvironment of tocopherol in the hydrophobic membrane. These two characteristic peaks obtained from the absorption and fluorescence spectra

have been used for determining the position of α-Toc in the membrane. The absorption maximum of α-Toc in PC is found at 296 nm, and this position is held within a wide concentration range.

Fig. 1A shows the fluorescence intensity changes recorded at the peak maximum, 325 nm, versus the total amount of α-Toc added to the sample. This dependence shows a linear relationship between the fluorescence intensity and the concentration of α-Toc incorporated into PC vesicles. At both PC concentrations, the dependence is similar. At the beginning, the linear fluorescence increase reaches a maximum at 22 mol% in 0.2 mg/ml PC and at 17 mol% in 2 mg/ml PC. Any further α-Toc concentration increase gradually reduces the fluorescence intensity.

At low tocopherol concentrations, there is no change in either the peak position or the spectrum shape, and no deposition is found on the cuvette. As α-Toc is practically insoluble in water, the recorded fluorescence can be assumed to arise mainly from the monomeric form of α-Toc embedded into the PC bilayer. At higher tocopherol concentrations, fluorescence quenching is observed. This may be associated with the formation of tocopherol dimers or aggregates. However, the fluorescence arising from the α-Toc dimer is much weaker than that arising from the monomer. The observed concentration-dependent fluorescence quenching suggests that the emission originates from the structures with high local α-Toc concentrations and may arise from the tocopherol domains forming in the membrane.

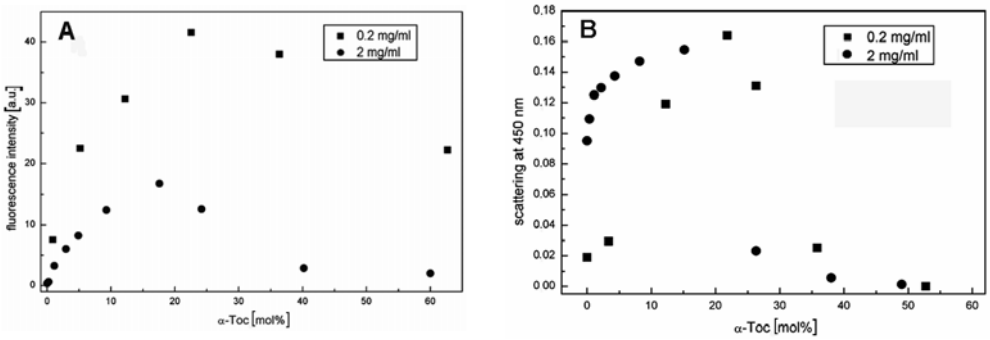

Fig. 1. The α-Toc concentration dependence in a 0.2 mg/ml and 2 mg/ml PC membrane as A – fluorescence recorded at 325 nm with excitation at 296 nm, B – turbidity measured at 450 nm. The key is provided in the insets.

Turbidity measurements

Turbidity measurements are often used as a crude tool to determine the size of the scattering particles. In the case of membranes, an increase in turbidity or light scattering is interpreted as an increase in the size of the vesicles.

This method was applied to estimate the changes in vesicle size. Fig. 1B shows the turbidity *vs.* α-Toc concentration. The scattering value without α-Toc in the sample indicates that the size of the PC vesicle depends on the initial lecithin

concentration. Increasing the amount of added α-Toc increases the scattering amplitude. In the 0.2 mg/ml PC sample, the scattering maximum is observed at 22 mol%. Above that concentration, the turbidity is found to decrease rapidly, and at 50 mol%, the sample is transparent. In the sample with 2 mg/ml PC, the scattering maximum is found at 15 mol%. At higher α-Toc concentrations, the scattering decreases to a very low level and becomes transparent at 50 ml%.

The initial increase in scatter reflects vesicle merging induced by the addition of α-Toc. Also, the maximum size of the vesicle formed in the presence of α-Toc is found not to depend on the initial lecithin concentration, but the position of the maximum depends on the α-Toc/PC ratio.

The turbidity results suggest that the presence of α-Toc induces structural changes in the membrane. The increasing amount of α-Toc in the membrane initially induces the formation of larger vesicles. When this process continues with α-Toc above 20 mol%, one can observe membrane disruption and collapse of the large vesicle, followed by the formation of smaller vesicles or mixed micelles.

Fluorescence quenching studies

External quenchers, through their collisions with fluorophore, will reflect the changes in its accessibility under specific conditions. The fluorescence quenching technique was applied to obtain information on the position of the α-Toc in the membrane. Additionally, this method was used to deduce structural changes in the vesicles in the presence of α-Toc. In these studies, non-penetrating $CuSO_4$, ionic potassium iodide (KI) and neutral acrylamide (ACR) were used as quenchers of tocopherol fluorescence in the presence of the PC membrane. KI and ACR are aqueous phase quenchers, and both can penetrate the membrane at a similar rate [31].

The quenching experiments were conducted at 15 mol% and 50 mol% α-Toc concentrations in the PC membrane, revealing a fluorescence maximum and a minimum, respectively (see Fig. 1A). The results obtained at 15 mol% α-Toc are presented as Stern-Volmer plots in Fig. 2. Acrylamide, the neutral polar quencher, shows a similar quenching rate at both membrane concentrations with $K_{SV} = 10.5\ M^{-1}$. At a quencher concentration above 100 mM, the Stern-Volmer plot shows an upward curvature for both PC concentrations. Such a feature suggests the mechanism of dynamic and static quenching. Static quenching of fluorescence may arise from the ground state complex formation between acrylamide and tocopherol. This complex should be evident from the absorption spectrum of tocopherol as acrylamide was added, but no changes in the absorption spectrum were observed up to an acrylamide concentration of 0.5 M in the sample. In order to explain the upward curvature, another approach, referred to as the "sphere of action" model, was applied [32]. In this mechanism, fluorophore quenching is assumed to be complete if a quencher molecule Q is inside a sphere (called the sphere of effective quenching, the active sphere or the

quenching sphere) of volume V[Q], surrounding the fluorophore M. If a quencher is beyond the active sphere, it has no effect on M at all. Therefore, the fluorescence intensity of the solution decreases with an increasing number of quenchers Q.

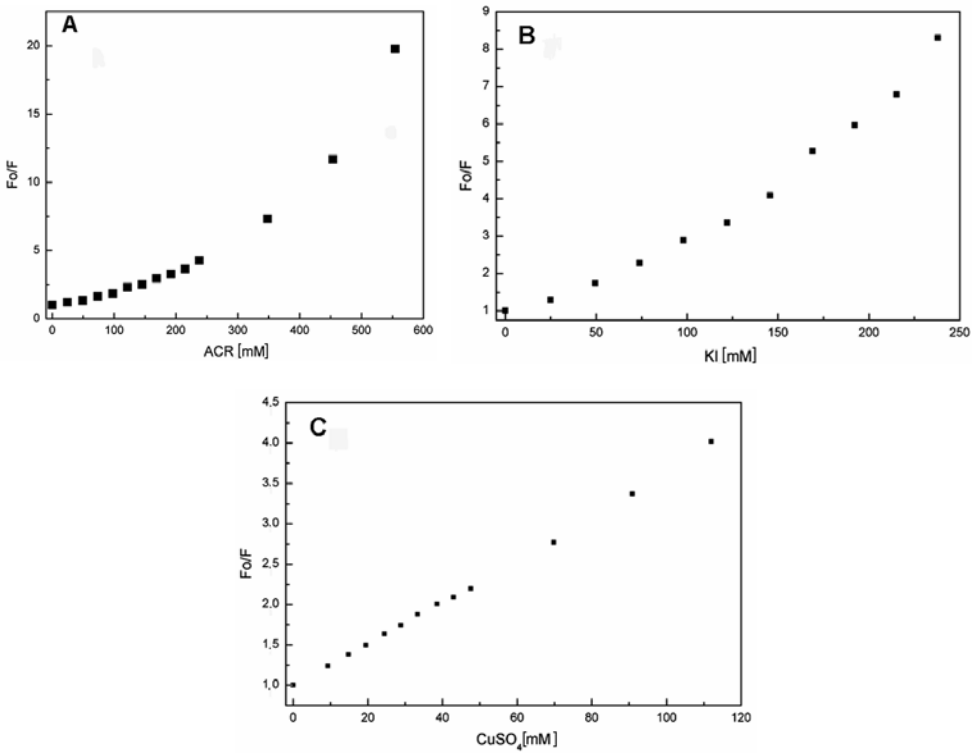

Fig. 2. Fluorescence quenching of 15 mol% α-Toc in 0.2 mg/ml PC by A – acrylamide, B – iodide, C – $CuSO_4$.

This mechanism leads to the modified Stern-Volmer equation (1):

$$\frac{F_0}{F\exp(V[Q])} = 1 + K_D[Q] \qquad (1)$$

where: F and F_0 denote the fluorescence intensity with and without the quencher Q, respectively; K_D is the dynamic quenching constant; and V is the static quenching constant.

In order to determine the acrylamide-quenching parameters of α-Toc in this mechanism, the modified Stern-Volmer equation (1) was applied with two fitting parameters, K_D and V. The static quenching constant V represents an

active volume surrounding the excited fluorophore. It is then possible to calculate the radius of the reaction distance R; the calculation results are shown in Tab. 1.

As the Stern-Volmer plot obtained for KI exhibits an upward curvature at both membrane concentrations, kinetic quenching parameters were analyzed with the modified Stern-Volmer equation (1). The fitted results are presented in Tab. 1. The Stern-Volmer plot of the aqueous phase cationic quencher $CuSO_4$ shows a linear dependence, which allowed the calculation of the Stern-Volmer quenching constant K_{SV}, also given in Tab. 1. It is noteworthy that the dynamic quenching constant values calculated for the ionic quencher are much higher than those obtained for neutral acrylamide. Additionally, the quenching constant for both charged quenchers in the 0.2 mg/ml PC membrane is higher than in that of 2 mg/ml concentration.

At high α-Toc concentration (50 mol% in the sample), the fluorescence intensity is low and the presence of 5 mM of ACR or KI quenches fluorescence to a barely measurable level. Such efficient quenching suggests that α-Toc in the newly formed structure is more accessible to the aqueous phase quenchers than it is in the membrane.

Tab. 1. Dynamic K_D, static V and Stern-Volmer K_{SV} quenching constant and radius of action R of 15 mol% α-Toc in PC membrane calculated from equation (1).

PC membrane	ACR			KI			$CuSO_4$
mg/ml	K_D [M^{-1}]	V [M^{-1}]	R [nm]	K_D [M^{-1}]	V [M^{-1}]	R [nm]	K_{SV} [M^{-1}]
0.2	6.2 ± 0.1	3.5 ± 0.1	1.12	43.1 ± 0.1	9.9 ± 0.1	9.83	28.4
2	6.3 ± 0.1	3.9 ± 0.1	1.18	13.1 ± 0.1	3.5 ± 0.1	1.12	11.9

The α-Toc fluorescence originates from the chromanol part of the tocopherol molecule. In the membrane, the tocopherol's "head" is located in a more polar region in the vicinity of a phosphate group, an anionic moiety of a phospholipid. Observed at both membrane concentrations, the efficient quenching by the charged quenchers indicates that electrostatic factors play a role in the interaction between α-Toc and the quencher in the lipid membrane. The parameters calculated for 0.2 mg/ml PC show about three-fold higher values compared to the 2 mg/ml concentration. This may suggest that in 0.2 mg/ml PC, the distance between polar heads is bigger, so it is possible that one quencher associates simultaneously with three fluorescent molecules. The possibility of such interaction in lipid membranes has already been reported [33]. The applied sphere of action model used in our calculations of V and R for ACR and KI quenching of α-Toc in the membrane yields values comparable with those reported by Zheng [34]. Also, the fact that no spectrum modifications were found indicates that no specific interactions between the fluorophore and the quenchers occur. When α-Toc is buried deeper in the bilayer, the access of the

quencher is limited [35]. Efficient quenching should occur in the structures where the chromanol part of tocopherol is exposed to external aqueous phase quenchers. Such unlimited access is possible when α-Toc is protruding from micelles, mixed micelles or non-lamellar structures, while the phytol chain is anchored in the hydrophobic part of the structure. Thus, besides the numerical values describing the quenching process, the results of the quenching experiments may indicate structural changes in the vesicles induced by the presence of α-Toc.

Dynamic light scattering (DLS)

The dynamic light scattering method has been extensively used for particle size analysis in the submicrometer range. It covers the size range of about 1 nm to 3 μm [29]. We applied the DLS method to calculate the size distribution of the PC vesicles formed in aqueous solution with and without tocopherol added. Fig. 3 shows the number-weighted hydrodynamic radius distribution of 2 mg/ml PC vesicles formed without, with 15 mol%, and with 60 mol% α-Toc in the sample.

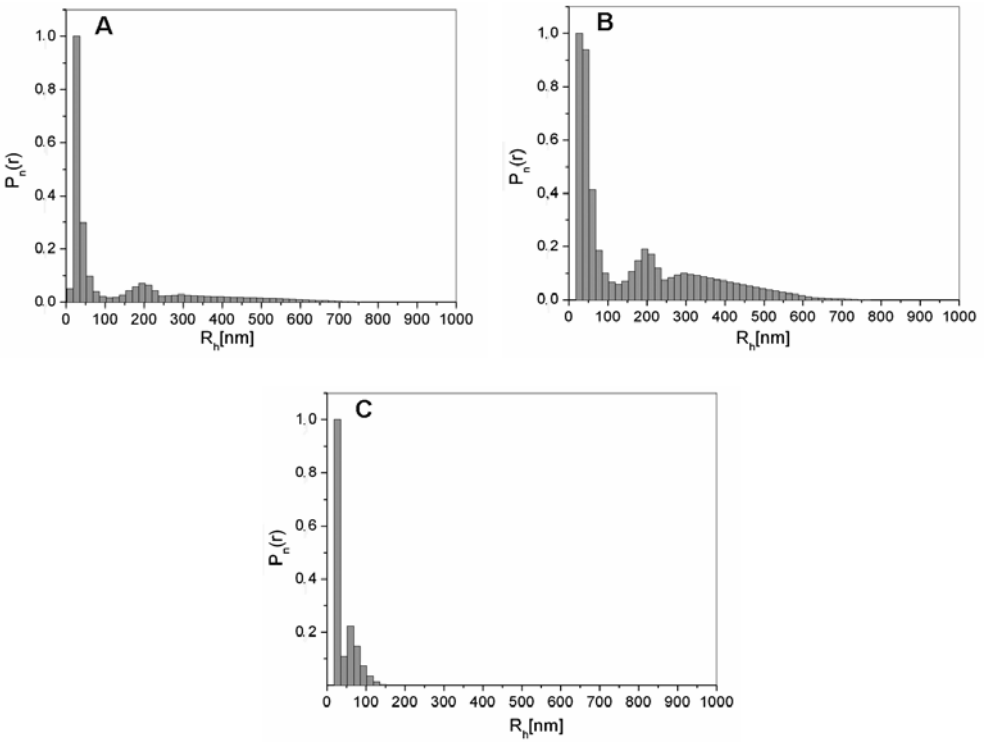

Fig 3. Weight-averaged diameter of the vesicles represented as a function of the mol fraction of α-Toc in 2 mg/ml PC. A – no α-Toc, B – 15 mol% α-Toc, C – 60 mol% α-Toc.

The α-Toc concentrations used refer to the maximum and minimum fluorescence observed at 15 mol% and at 60 mol%, respectively. According to Fig. 3A, there is a wide distribution of vesicle sizes from 20 nm up to 650 nm in the PC sample. However, vesicles of dimensions up to 250 nm constitute 95% of the total liposome population, with the maximum number of vesicles observed at a diameter of 35 nm. The presence of the 15 mol% α-Toc in the sample affects the distribution of the hydrodynamic radius of the vesicles. As can be seen in Fig. 3B, the number of the vesicles with greater radius increases. In the distribution curve for 60 mol% α-Toc concentration in the sample (Fig. 3C), the sizes of the formed structures range from 30 to 120 nm with a mean diameter of 60 nm, and no vesicles with a diameter above 120 nm are found. Similar results were obtained for the 0.2 mg/ml PC membrane.

In order to assign the obtained distributions to the proper structures, the numerical diameter values for those structures are indispensable. Another approach was used for this purpose, assuming that the scattering is due to three structures with different diameters. For the calculations using the *Discreete* program, a three-exponential function was assumed. In the 2 mg/ml sample with and without α-Toc, the first calculated component yielded a radius between 15 and 20 nm, which indicates the SSBV structure. The second component, with a radius of about 84 nm in all three samples, indicates the SUV. The formation of SUV in the range from 80 to 100 nm was observed in tocopherol-enriched PC liposomes [36]. For the third component, radius values of 553 nm, 334 nm and 270 nm were obtained, corresponding to samples without and with an increasing amount of α-Toc. The last component can be assigned to LUV or MLV. The contribution to the total scattering intensity of each component depends on the tocopherol concentration in the sample. The calculated diameters R and the contribution of each component to the scattering intensity are presented in Tab. 2.

Tab. 2. The calculated diameters R (nm) obtained using the *Discreete* program and the contribution (%) of each component to the total scattering intensity.

α -Toc	0		15 mol%		60 mol%	
	R [nm]	%	R [nm]	%	R [nm]	%
Micelle	15	5	20	8	15	< 1
SUV	84	45	82	53	84	88
LUV/MLV	533	50	334	37	270	12

It should be kept in mind that the amplitude of the decay time distribution in the scattering experiment is proportional to the sixth power of the particle radius and to the number of particles; the latter holds for spherical particles [29]. Hence, even a single large structure may contribute more to the total scattered intensity than a large number of small ones. This is clearly seen when we compare the data in Fig. 3A and that in Tab. 2 for the PC membrane. The distribution curve

shows the maximum number of structures of smaller radius around 60 nm, whereas the calculations indicate that 50% of the scattering contribution arises from a 533-nm structure. The same considerations are valid for the data presented in Fig. 3 and Tab. 2. Another source of the discrepancy between those two methods may reflect the fact that the observed structures do not possess radial symmetry and are not lamellar structures.

The DLS measurements have shown that increasing α-Toc concentration in the PC membrane decreases vesicle diameter, finally leading to its disruption and to the formation of new structures like mixed micelles or small lamellar vesicles. A presentation of the results as diameter distribution, as in Fig. 3, seems more adequate than the numerical diameter values of the structures shown in Tab. 2.

Optical microscopy

The images of lecithin giant vesicles obtained by optical microscopy are shown in Fig. 4. The pictures show unilamellar and multilamellar vesicles in the form of spheres of size ranging from 5 to 40 micrometers, depending on the components present in the system. The vesicles formed from 2 mg/ml PC are more uniform and do not exceed 15 micrometers, while those formed with the presence of 15 mol% α-Toc are larger, with diameters up to 40 micrometers. Their shapes differ considerably, being circular, oblate, unilamellar and multilamellar. The vesicles often have a few smaller unilamellar liposomes trapped inside. The variety of the shapes of the vesicles with and without α-Toc is a manifestation of structurally induced fluctuations leading to a new equilibrium. No vesicles were seen in the presence of 60 mol% of α-Toc in the sample, which suggests that the diameters of the newly formed structures are in the submicrometer range, not observable with an optical microscope.

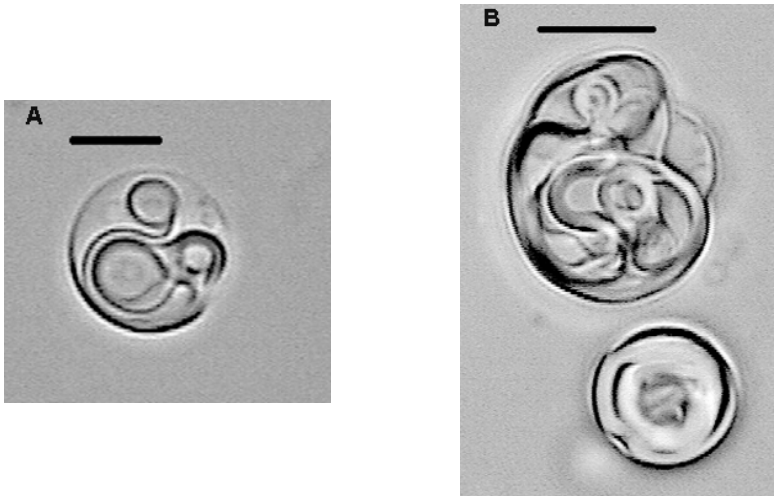

Fig. 4. The characteristic images of giant vesicles formed in a 2 mg/ml PC membrane without α-Toc (A) and in the presence of 15 mol% α-Toc (B). The bar length is 10 μm in both images.

No vesicles in any 0.2 mg/ml PC sample, with or without α-Toc, could be found with the optical microscope. It seems that at low PC concentrations, the formation of giant vesicles is energetically unfavorable and occurs very rarely.

DISCUSSION

The formation of vesicles in aqueous solutions is a common property observed in both artificial and naturally occurring phospholipids. Based on the knowledge of the structure of lipids present in PC, lamellar (vesicular) and micellar phases could be expected. The results of this study, using dynamic light scattering, turbidometry and optical microscopy methods, show that in aqueous solutions, the amphiphilic properties of PC lead to the formation of supramolecular aggregates, ranging in size from small single-bilayer vesicles and small unilamellar vesicles to giant multilamellar vesicles. This occurs as a result of dynamic intermolecular interactions that exist within a single phase [37]. It is known that the size of the formed vesicles depends on Laplace pressure, interfacial tension, concentration, temperature and the presence of other components. The physical stability of the vesicles depends on the thermal mobility of the components and may lead to the formation of larger vesicles or to the assembling of smaller vesicles. The driving force of those processes is the reduction in the Gibbs free energy (ΔG) of interface tension; introducing another component to the system may be expected to affect the thermodynamic equilibrium, resulting in morphological and structural changes. The α-Toc fluorescence, DLS and turbidometric data presented in Fig. 1 and Fig. 3 indicate that at low concentrations, below 15 mol%, α-Toc is embedded into the membrane in the monomeric form in a rather statistical manner. At the same time, an increase in the vesicle size was observed. This suggests that increasing tocopherol concentration in the membrane affects the lipophyllic balance, causing the formation of larger vesicles. Changes in the membrane structure in the presence of tocopherol have been reported in experiments using other methods as well. The formation of ripple phases in the phospholipid membrane at 5 mol% tocopherol concentration in saturated phosphatidylcholines was reported in X-ray diffraction and freeze-fracture electron microscopic studies. In the presence of more than 10 mol% α-tocopherol, biplanar bilayers with a worm-like surface texture were observed. Thus, α-tocopherol-enriched domains induce ripple phases with long-range and short-range periodicity. Planar bilayers with an increasing proportion of α-tocopherol in the mixtures (up to 20 mol%) were observed as well [10]. Impedance spectroscopy studies of α-Toc/PC mixtures with increasing tocopherol concentration, up to 46 mol%, are reported to show the condensation effect of tocopherol in the PC membrane and the formation of domains with 10:1 stoichiometry [15].

The non-linear fluorescence increase combined with further fluorescence-quenching behavior observed above 20 mol% (Fig. 1A) indicates the formation of tocopherol-enriched domains in the membrane. The simultaneous decrease in

turbidity, optical microscopy data and DLS have shown that at α-Toc mole fractions in the membrane higher than 20 mol%, a decrease in vesicle size occurred. All those results suggest morphological and structural changes to the vesicles. Other results which indicate that tocopherol in the membrane is not distributed randomly in similar systems have been published as well [12, 38, 39]. The 20 mol% value is very probably related to the limited solubility of α-Toc in phospholipid bilayers, whereas the disintegration of the membrane indicates a rapid change in the hydrophyllic-lipophyllic balance, bringing about the formation of non-lamellar structures. The formation of hexagonal H_{II} or reversed cubic phases due to incorporated α-Toc was observed in DPPC or DPPE membranes [10, 40-42].

Microscopic and particle size measurements indicate that the presence of tocopherol with a molar ratio above 0.2 resulted in the effective formation and stabilization of submicrometer size vesicles. Complexes between tocopherol and fatty acids are known to occur in organic solvents [43-47]. The formation of such lipid/α-Toc complexes with different stoichiometry has been revealed by X-ray diffraction studies, as well as by fluorescence in both the gel and fluid phases of phospholipid membranes [45, 48-55]. The above-cited references and the obtained data lead to the formulation of the following mechanism. Phospholipid relocation from the vesicles to the aqueous dispersed phase occurs within the sample during homogenation with the subsequent formation of specific mixed SUV, micelles or other type of aggregates. The fluorescence quenching data shows that tocopherol-stabilized vesicles are composed of small liposomes, micelles and aggregates of both. The size of the liposomes formed covers the range from 20 to 120 nm. It seems that the formation of new structures is not reversible. If aggregated, they mostly maintain their initial shape and size for at least one week. This indicates an interaction of the phospholipids with the tocopherol molecules, with a possible effect on their stability and an inhibiting impact on the formation of the lamellar vesicles.

The protective antioxidant role of tocopherol is played by a monomeric molecule of α-tocopherol, which undergoes further transformations during oxidation. The presented results indicate that the number of tocopherol molecules that may be incorporated into the membrane as a monomer is limited. The spectroscopic parameters of α-Toc determined in this study indicate that the α-Toc monomer is included into the hydrophilic part of the PC membrane. [56]. Increasing tocopherol concentration in the membrane leads to self-quenching of the α-Toc fluorescence. On the molecular level, the observed phenomena can be ascribed to the interactions between α-Toc molecules and membrane phospholipids. The formation of exciplexes or ground-state complexes between tocopherol and fatty acids has been confirmed in studies using EPR [55] and fluorescence [9, 49, 57, 58] methods. Very probably, the formation of complexes between α-Toc methyl groups attached to the aromatic ring of the chromanol moiety and either free fatty acids or fatty acids esterified to the sn-2 position of PCs occurs in the

investigated system. The structure and morphology of the aggregates formed in the PC membrane, whether those are mixed micelles or multilamellar layers of phospholipids covering micelles or the opposite, is currently under investigation. The presented view on the disruption process at high tocopherol concentrations in the membrane, compared to X-ray, freeze-fracture microscopy, NMR or impedance spectroscopy, arises from the fact that fluorescence is a very local method, covering a microenvironment with a radius of about 1 nm. This allows us to determine the type of interactions between components of the system, though at the expense of the micrometer-sized approach, lost to observe submicrometer domains of lipid-tocopherol mixtures.

In conclusion, the results obtained indicate that the hydrophilic-lipophilic balance in neutral bilayers formed from partially unsaturated lipids is upset when a substantial amount of α-Toc is introduced. This in turn induces a disruption process which finally leads to the formation of small vesicles and non-lamellar structures like micelles or mixed micelles.

Acknowledgments. This study was partially supported by a grant from the Polish Scientific Council, KBN 2 P06T 016 27. We gratefully acknowledge the technical assistance at work with optical microscope of Dr Hanna Jackowiak from the Department of Animal Anatomy, Agricultural University in Poznań.

REFERENCES

1. Ortiz, A., Aranda, F.J. and Gomez-Fernandez, J.C. A differential scanning calorimetry study of the interaction of alpha-tocopherol with mixtures of phospholipids. **Biochim. Biophys. Acta** 898 (1987) 214-222.
2. Ortiz, A., Villalain, J. and Gomez-Fernandez, J.C. Interaction of diacylglycerols with phosphatidylcholine vesicles as studied by differential scanning calorimetry and fluorescence probe depolarization. **Biochemistry** 27 (1988) 9030-9036.
3. Walke, M., Beckert, D. and Lasch, J. Interaction of UV light-induced alpha-tocopherol radicals with lipids detected by an electron spin resonance prooxidation effect. **Photochem. Photobiol.** 68 (1998) 502-510.
4. Aranda, F.J., Sanchez-Migallon, M.P. and Gomez-Fernandez, J.C. Influence of alpha-tocopherol incorporation on Ca(2+)-induced fusion of phosphatidylserine vesicles. **Arch. Biochem. Biophys.** 333 (1996) 394-400.
5. Grau, A. and Ortiz, A. Dissimilar protection of tocopherol isomers against membrane hydrolysis by phospholipase A2. **Chem. Phys. Lipids** 91 (1998) 109-118.
6. Gutierrez, M.E., Garcia, A.F., Africa de Madariaga, M., Sagrista, M.L., Casado, F.J. and Mora, M. Interaction of tocopherols and phenolic compounds with membrane lipid components: evaluation of their antioxidant activity in a liposomal model system. **Life Sci.** 72 (2003) 2337-2360.

7. Chen, C.S., Patterson, M.C., Wheatley, C.L., O'Brien, J.F. and Pagano, R.E. Broad screening test for sphingolipid-storage diseases. **Lancet** 354 (1999) 901-905.
8. Nacka, F., Cansell, M., Meleard, P. and Combe, N. Incorporation of alpha-tocopherol in marine lipid-based liposomes: in vitro and in vivo studies. **Lipids** 36 (2001) 1313-1320.
9. Stillwell, W., Ehringer, W. and Wassall, S.R. Interaction of alpha-tocopherol with fatty acids in membranes and ethanol. **Biochim. Biophys. Acta** 1105 (1992) 237-244.
10. Chen, H.W., Chiang, T., Wang, C.Y. and Lii, C.K. Inhibition of tert-butyl hydroperoxide-induced cell membrane bleb formation by alpha-tocopherol and glutathione. **Food Chem. Toxicol.** 38 (2000) 1089-1096.
11. Sezer, A.D., Bas, A.L. and Akbuga, J. Encapsulation of enrofloxacin in liposomes I: preparation and in vitro characterization of LUV. **J. Liposome Res.** 14 (2004) 77-86.
12. Quinn, P.J. Characterisation of clusters of alpha-tocopherol in gel and fluid phases of dipalmitoylglycerophosphocholine. **Eur. J. Biochem.** 233 (1995) 916-925.
13. Wang, X., Semmler, K., Richter, W. and Quinn, P.J. Ripple phases induced by alpha-tocopherol in saturated diacylphosphatidylcholines. **Arch. Biochem. Biophys.** 377 (2000) 304-314.
14. Massey, J.B. Interfacial properties of phosphatidylcholine bilayers containing vitamin E derivatives. **Chem. Phys. Lipids** 109 (2001) 157-174.
15. Naumowicz, M. and Figaszewski, Z.A. Impedance analysis of phosphatidyl-choline/alpha-tocopherol system in bilayer lipid membranes. **J. Membr. Biol.** 205 (2005) 29-36.
16. Kaasgaard, T., Mouritsen, O.G. and Jorgensen, K. Lipid domain formation and ligand-receptor distribution in lipid bilayer membranes investigated by atomic force microscopy. **FEBS Lett.** 515 (2002) 29-34.
17. Leidy, C., Mouritsen, O.G., Jorgensen, K. and Peters, G.H. Evolution of a rippled membrane during phospholipase A2 hydrolysis studied by time-resolved AFM. **Biophys. J.** 87 (2004) 408-418.
18. Pedersen, T.B., Kaasgaard, T., Jensen, M.O., Frokjaer, S., Mouritsen, O.G. and Jorgensen, K. Phase behavior and nanoscale structure of phospholipid membranes incorporated with acylated C14-peptides. **Biophys. J.** 89 (2005) 2494-2503.
19. Menger, F.M. and Keiper, J.S. Chemistry and physics of giant vesicles as biomembrane models. **Curr. Opin. Chem. Biol.** 2 (1998) 726-732.
20. Asai, Y. Structural differences in aqueous dispersions of alpha-tocopheryl acetate and phosphatidylcholine upon varying their molar fractions. **Pharmazie** 59 (2004) 849-853.
21. Gramlich, G., Zhang, J. and Nau, W.M. Diffusion of alpha-tocopherol in membrane models: probing the kinetics of vitamin E antioxidant action by fluorescence in real time. **J. Am. Chem. Soc.** 126 (2004) 5482-5492.

22. Pandey, B.N. and Mishra, K.P. Effect of radiation induced lipid peroxidation on diphenylhexatriene fluorescence in egg phospholipid liposomal membrane. **J. Biochem. Mol. Biol. Biophys.** 6 (2002) 267-272.
23. Naguib, Y.M. A fluorometric method for measurement of peroxyl radical scavenging activities of lipophilic antioxidants. **Anal. Biochem.** 265 (1998) 290-298.
24. Di Giulio, A., Saletti, A., Oratore, A. and Bozzi, A. Monitoring by cis-parinaric fluorescence of free radical induced lipid peroxidation in aqueous liposome suspensions. **J. Microencapsul.** 13 (1996) 435-445.
25. LaLonde, R.T. and Xie, S. Glutathione and N-acetylcysteine inactivations of mutagenic 2(5H)-furanones from the chlorination of humics in water. **Chem. Res. Toxicol.** 6 (1993) 445-451.
26. Benezra, C., Sigman, C.C., Perry, L.R., Helmes, C.T. and Maibach, H.I. A systematic search for structure-activity relationships of skin contact sensitizers: methodology. **J. Invest. Dermatol.** 85 (1985) 351-356.
27. Kuksis, A. Animal lecithins. **J. Am. Oil Chem. Soc. USA** 12 (1985) 105-162.
28. Gennis, R.B. Biomembranes: molecular structure and function in Membranes. Springer-Verlag: New York, 1989.
29. Berne, R. and Pecora, R. Dynamic Light Scattering. New York: Wiley 1976.
30. Eastman, S.J., Hope, M.J. and Cullis, P.R. Transbilayer transport of phosphatidic acid in response to transmembrane pH gradients. **Biochemistry** 30 (1991) 1740-1745.
31. Moro, F., Goni, F.M. and Urbaneja, M.A. Fluorescence quenching at interfaces and permaetion of acrylamide and iodide across phospholipid bilayers. **FEBS** 330 (1993) 129-132.
32. Eftink, M.R. and Ghiron, C.A. Fluorescence quenching of indole and model micelle systems **J. Phys. Chem.** 80 (1976) 486-492.
33. Kalinin, S.V. and Molotkovsky, J.G. Anion binding to lipid bilayers: determination using fluorescent membrane probe by direct quenching or by competitive displacement approaches. **J. Biochem. Biophys. Methods** 46 (2000) 39-51.
34. Zheng, B., Wu, J.N., Schober, W., Lewis, D.E. and Vida, T. Isolation of yeast mutants defective for localization of vacuolar vital dyes. **Proc. Natl. Acad. Sci. USA** 95 (1998) 11721-11726.
35. Fukuzawa, K., Ikebata, W. and Sohmi, K. Location, antioxidant and recycling dynamics of alpha-tocopherol in liposome membranes. **J. Nutr. Sci. Vitaminol. (Tokyo)** 39 Suppl (1993) S9-22.
36. Ferezou, J., Nguyen, T.L., Leray, C., Hajri, T., Frey, A., Cabaret, Y., Courtieu, J., Lutton, C. and Bach, A.C. Lipid composition and structure of commercial parenteral emulsions. **Biochim. Biophys. Acta** 1213 (1994) 149-158.
37. Chungcharoenwattana, S. and Ueno, M. Size control of mixed egg yolk phosphatidylcholine (EggPC)/oleate vesicles. **Chem. Pharm. Bull. (Tokyo)** 52 (2004) 1058-1062.

38. Wang, X. and Quinn, P.J. Preferential interaction of alpha-tocopherol with phosphatidylcholines in mixed aqueous dispersions of phosphatidylcholine and phosphatidylethanolamine. **Eur. J. Biochem.** 267 (2000) 6362-6368.
39. Wang, X. and Quinn, P.J. The interaction of alpha-tocopherol with bilayers of 1-palmitoyl-2-oleoyl-phosphatidylcholine. **Biochim. Biophys. Acta** 1567 (2002) 6-12.
40. Nakajima, K., Utsumi, H., Kazama, M. and Hamada, A. Alpha-tocopherol-induced hexagonal HII phase formation in egg yolk phosphatidylcholine membranes. **Chem. Pharm. Bull. (Tokyo)** 38 (1990) 1-4.
41. Chudinova, V.V., Zakharova, E.I., Alekseev, S.M., Chupin, V.V. and Evstigneeva, R.P. [Study of the interaction of alpha-tocopherol with phospholipids, fatty acids, and their oxygenated derivatives by (31)P-NMR spectroscopy]. **Bioorg. Khim.** 19 (1993) 243-249.
42. Bagatolli, L.A. and Gratton, E. Two photon fluorescence microscopy of coexisting lipid domains in giant unilamellar vesicles of binary phospholipid mixtures. **Biophys. J.** 78 (2000) 290-305.
43. Erin, A.N., Spirin, M.M., Tabidze, L.V. and Kagan, V.E. [Formation of alpha-tocopherol complexes with fatty acids. Possible mechanism of biomembrane stabilization by vitamin E]. **Biokhimiia** 48 (1983) 1855-1861.
44. Erin, A.N., Spirin, M.M., Tabidze, L.V. and Kagan, V.E. Formation of alpha-tocopherol complexes with fatty acids. A hypothetical mechanism of stabilization of biomembranes by vitamin E. **Biochim. Biophys. Acta** 774 (1984) 96-102.
45. Kagan, V.E. and Quinn, P.J. The interaction of alpha-tocopherol and homologues with shorter hydrocarbon chains with phospholipid bilayer dispersions. A fluorescence probe study. **Eur. J. Biochem.** 171 (1988) 661-667.
46. Urano, S., Shichita, N. and Matsuo, M. Interaction of vitamin E and its model compounds with unsaturated fatty acids in homogeneous solution. **J. Nutr. Sci. Vitaminol. (Tokyo)** 34 (1988) 189-194.
47. Chudinova, V.V., Zakharova, E.I., Alekseev, S.M. and Evstigneeva, R.P. [Interaction of vitamin E (alpha-tocopherol) with oxygenated fatty acid derivatives]. **Bioorg. Khim.** 19 (1993) 505-511.
48. Salgado, J., Villalain, J. and Gomez-Fernandez, J.C. Alpha-tocopherol interacts with natural micelle-forming single-chain phospholipids stabilizing the bilayer phase. **Arch. Biochem. Biophys.** 306 (1993) 368-376.
49. Bourgeois, C.F., George, P.R. and Cronenberger, L.A. Automated determination of alpha-tocopherol in food and feed. Part 2. Continuous flow technique. **J. Assoc. Anal. Chem.** 67 (1984) 631-634.
50. Tiurin, V.A., Kagan, V.E., Serbinova, E.A., Gorbunov, N.V. and Erin, A.N. [The interaction of alpha-tocopherol with phospholipid liposomes: the absence of transbilayer mobility]. **Biull. Eksp. Biol. Med.** 102 (1986) 689-692.

51. Urano, S., Iida, M., Otani, I. and Matsuo, M. Membrane stabilization of vitamin E; interactions of alpha-tocopherol with phospholipids in bilayer liposomes. **Biochem. Biophys. Res. Commun.** 146 (1987) 1413-1418.
52. Urano, S., Yano, K. and Matsuo, M. Membrane-stabilizing effect of vitamin E: effect of alpha-tocopherol and its model compounds on fluidity of lecithin liposomes. **Biochem. Biophys. Res. Commun.** 150 (1988) 469-475.
53. Wassall, S.R., Phelps, T.M., Wang, L.J., Langsford, C.A. and Stillwell, W. Membrane stabilization by vitamin E: magnetic resonance studies of the interaction of alpha-tocopherol with fatty acid acyl chains in phospholipid model membranes. **Prog. Clin. Biol. Res.** 292 (1989) 435-444.
54. Wang, X. and Quinn, P.J. Vitamin E and its function in membranes. **Prog. Lipid. Res.** 38 (1999) 309-336.
55. Srivastava, S., Phadke, R.S. and Govil, G. Effect of incorporation of drugs, vitamins and peptides on the structure and dynamics of lipid assemblies. **Mol. Cell. Biochem.** 91 (1989) 99-109.
56. Bellemare, F. and Fragata, M. Transmembrane distribution of alpha-tocopherol in single-lamellar mixed lipid vesicles. **J. Membr. Biol.** 58 (1981) 67-74.
57. Kagan, V.E., Bakalova, R.A., Serbinova, E.E. and Stoytchev, T.S. Fluorescence measurements of incorporation and hydrolysis of tocopherol and tocopheryl esters in biomembranes. **Methods Enzymol.** 186 (1990) 355-367.
58. Bally, M.B., Mayer, L.D., Loughrey, H., Redelmeier, T., Madden, T.D., Wong, K., Harrigan, P.R., Hope, M.J. and Cullis, P.R. Dopamine accumulation in large unilamellar vesicle systems induced by transmembrane ion gradients. **Chem. Phys. Lipids** 47 (1988) 97-107.